第36卷第9期 2020年9月
无 机 化 学 学 报 CHINESE JOURNAL OF INORGANIC CHEMISTRY
Vol.36 No.9 1783-1790

吡啶类单核钴(Ⅱ)配合物的合成、结构、与DNA的相互作用及细胞毒性

高春艳[#,*,1] 乔佩佩[#,1] 杨皇泽[1] 张鹏飞[1] 雷云博[1]
张永坡[1] 王 敏[2] 岳爱琴[2] 赵晋忠[1] 杜维俊[*,2]
([1]山西农业大学基础部,晋中 030801)
([2]山西农业大学农学院,晋中 030801)

摘要: 合成了一个新的单核钴配合物[Co(L)Cl_2],配体L为吡啶类多齿配体4-甲基-*N*,*N*-二(吡啶-2-亚甲基)苯胺。对化合物进行了红外光谱、元素分析、X射线单晶衍射的表征。结果表明配合物的Co(Ⅱ)中心为五配位畸变的三角双锥构型。利用电子吸收、发射光谱和凝胶电泳等方法研究了配合物与DNA的相互作用。结果表明不加诱导剂时该配合物与DNA能表现出一定程度的切割活性,而加入诱导剂过氧化氢后,化学核酸酶活性显著提高。其切割机理为氧化切割机理,其中活性氧可能为·OH和$^1O_2$,且配合物与DNA的结合部位可能在大沟槽处。另外,用MTT实验测定了该配合物对体外HeLa、BGC-823、NCI-H460肿瘤细胞生长的抑制能力。

关键词: 钴配合物; 吡啶类配体; DNA键合; DNA切割; 细胞毒性
中图分类号: O614.81+2 **文献标识码:** A **文章编号:** 1001-4861(2020)09-1783-08
DOI: 10.11862/CJIC.2020.208

Synthesis, Structure, DNA interaction and Cytotoxicity of Pyridine-Based Mononuclear Cobalt(Ⅱ) Complex

GAO Chun-Yan[#,*,1] QIAO Pei-Pei[#,1] YANG Huang-Ze[1] ZHANG Peng-Fei[1] LEI Yun-Bo[1]
ZHANG Yong-Po[1] WANG Min[2] YUE Ai-Qin[2] ZHAO Jin-Zhong[1] DU Wei-Jun[*,2]
([1]*Department of Basic Sciences, Shanxi Agricultural University, Jinzhong, Shanxi* 030801, *China*)
([2]*College of Agronomy, Shanxi Agricultural University, Jinzhong, Shanxi* 030801, *China*)

Abstract: A new mononuclear complex [Co(L)Cl_2] (L=4-methyl-*N*,*N*-bis(pyridin-2-ylmethyl) aniline) was synthesized and characterized by infrared spectroscopy, elemental analysis and X-ray single crystal diffraction. The results show that the Co(Ⅱ) center of the complex is a distorted trigonal-bipyramidal configuration with N_3Cl_2 donor sets. The interaction between the complex and DNA was studied by the electron absorption, emission spectroscopy and gel electrophoresis. The results reveal that the complex bind to CT-DNA by partial intercalation binding mode, and in the presence of hydrogen peroxide as a inducer, the DNA cleavage abilities of the complex are significantly improved. The Oxidative mechanism has been demonstrated via the pathway involving both hydroxyl radicals (·OH) and singlet oxygen ($^1O_2$) as ROS, and the binding site between the complex and DNA may be in the large groove. In addition, *in vitro* cytotoxicity of the drug has been tested by MTT against HeLa, BGC-823 and NCI-H460 cell lines. CCDC: 1966237.

Keywords: cobalt(Ⅱ) complex; pyridine-based ligand; DNA binding; DNA cleavage; cytotoxicity

收稿日期:2020-03-07。收修改稿日期:2020-05-27。
山西省重点研发计划项目(No.201703D211001, 201903D221036, 201703D221008-4, 201703D221004-5)、山西省自然科学基金(No.201701D221157, 201701D221158)、山西农业大学引进人才科研启动金(No.2013YJ40)和山西省高等学校大学生创新创业训练项目(No.2019136, 2019137)资助项目。
[#]共同第一作者。
[*]通信联系人。E-mail:gaocynk@163.com, duweijun68@126.com;会员登记号:S06N2534M1605。

0 Introduction

DNA, the deoxyribonucleotide, is a major component of chromosomes and plays an important role in the translation, transcription and replication of the genetic code of life. Also, DNA is an important target molecule for many antitumor drugs *in vivo*[1]. In recent years, the interaction of small molecule transition metal complexes with DNA and its chemical nuclease activity has become a hot spot in bioinorganic chemistry research. Transition metal complexes have been widely used as DNA structure probes, DNA molecular light switches, DNA breaking agent and anticancer drugs[2-5]. In order to further explore the reaction mechanism of metal complexes and DNA interaction, people used copper, iron, zinc, ruthenium and other metals to synthesize a large number of metal complexes for research[6-9]. Spectroscopic studies suggest that there exists an interaction between acyclic copper complex of Cu(L) (H_2O) and DNA[10]. The dipyridine copper complexes with guanidine/amine side chains discovered by Ji Liang-Nian et al. can hydrolyze superhelix DNA and obtain linear products at the same time[11]. The ruthenium(Ⅲ) polypyridine complexes can intercalate into DNA base pairs, and it is found that single oxygen ($^1O_2$) is likely to be the ROS (reactive oxygen species) for catalytic cleavage[12]. The zinc(Ⅱ) complex containing guanidine thiosemicarbazide shows that it has certain anti-tumor cell proliferation *in vitro* for lung cancer cells (A549) and breast cancer cells (MCF7) through cytotoxicity experiments and its action may be combined into cell DNA by partial insertion[13].

Cobalt is an essential trace element found in all animals. Cobalt plays a crucial role in several biologically important processes, and is predominately found in the form of vitamin B12 (cobalamin). Many biological enzymes rely on the reaction of cobalt to stimulate their activity, so as to complete the catalytic effect on the metabolic process in the organism. The different forms of cobalamin are necessary for proper formation of red blood cells, DNA synthesis and regulation, and the maintenance of normal brain and nerve function. There is also evidence implicating cobalamin in fatty acid and amino acid metabolism. Given the prominent role of cobalt in biological processes, humans have evolved mechanisms to overcome cobalt overload. Cobalt is thus less toxic to humans than non-essential metals like platinum[14-16]. Therefore, the study of cobalt complexes is of great significance in pharmacology, coordination chemistry and bioinorganic chemistry

Herein, we synthesized a new cobalt complex and confirmed the crystal structure by X-ray single crystal diffractometer; further characterized the complex by infrared spectroscopy and elemental analysis; and interaction between the complex and CT-DNA were studied by electron absorption spectroscopy and fluorescence spectroscopy. The cleavage effect of the complex on the plasmid pBR322 DNA and its mechanism were studied by agarose gel electrophoresis. It provides preliminary work basis for the synthesis of chemical nucleases with DNA site-specific recognition and localization cleavage. Moreover, MTT method was used to determine the inhibitory effect of the complex on the growth of tumor cells *in vitro*.

1 Experimental

1.1 Instruments and reagents

Elemental analysis (C, H, N) was conducted with a PerkinElmer 240Q elemental analyzer. IR spectra were obtained on a Bruker TENOR 27 Fourier transform infrared spectrometer. Electronic spectra were measured on a JASCO V-570 spectrophotometer. Fluorescence spectrum was measured with a Cary Eclipse fluorescence spectrometer. The electrophoresis experiment was performed with constant pressure DYY-Ⅲ electrometer, and the gel imaging experiment was performed with UVITEC gel automatic imaging analysis system.

All reagents and solvents were purchased from commercial sources. The complex was soluble in H_2O-DMF mixed solvent, 0.01 mol·L^{-1} in 10%(*V*/*V*) DMF/H_2O of the stock solution was stored at 4 ℃ and prepared to required concentrations for the chemical nuclease and bioactivity experiments. Tris, EDTA, DMSO, NaCl and H_3BO_3 used in biological activity experiments are guarantee reagents. Calf thymus DNA

(CT-DNA) (BR) was produced by Fluka company. PBR322 DNA (BR) was purchased from Fermentas; ethidium bromide (EB) (AR) and agarose were Sigma-Aldrich products. Fetal bovine serum, RPMI1640, DMEM, and MTT were purchased from Solarbio.

1.2 Synthesis of [Co(L)Cl_2] (1)

The synthesis and characterization of ligand L (4-methyl-*N*,*N*-bis(pyridin-2-ylmethyl) aniline) refer to published literature[17-18]. The ligand (0.2 mmol) was dissolved in 10 mL methanol and stirred. At the same time, 0.2 mmol *N*, *N*-diethyl-ethylamine was added dropwise. After stirring at room temperature for 30 min, 10 mL $CoCl_2 \cdot 6H_2O$ (0.2 mmol, 26 mg) ethanol solution was slowly added, and the stirring was continued at room temperature for 5h. Then the mixture was filtered. The filtrate was allowed to stand at room temperature for one week until blue crystals suitable for X-ray collection was obtained. The excess solution was filtered, washed with ether, and dried in air. Yield: 38%. Element analysis Calcd. for $C_{19}H_{19}Cl_2CoN_3$(%): C, 54.44; H, 4.57; N, 10.02. Found(%): C, 54.49; H, 4.61; N, 9.99. FT-IR (KBr, cm^{-1}): 3 428, 3 068, 2 918, 1 608, 1 516, 1 482, 1 446, 1 310, 1 266, 1 191, 1 056, 1 025, 858, 816, 776, 650.

1.3 X-ray crystallography

The crystal with suitable size (0.4 mm×0.25 mm×0.2 mm) was selected for X-ray single crystal diffraction. X-ray diffraction data were collected on Bruker Smart 1000 CCD diffractometer using Mo $K\alpha$ radiation (λ=0.071 073 nm) with ω-2θ scan mode at 293(2) K[19]. The intensity data was corrected by the SADABS program. The crystal structure was obtained by direct method, and the full matrix least squares correction was performed on all non-hydrogen atoms by anisotropic thermal parameter method. Hydrogen atoms were added by geometric theoretical hydrogenation procedures. All calculations were done using the SHELXS-97 and SHELXL-97 programs[20-21]. Crystallographic data details and structure refinement parameters are presented in Table 1. Selected bond lengths and angles are listed in Table S1 (Supporting information).

CCDC: 1966237.

Table 1　Crystallographic data for complex 1

Molecular formula	$C_{19}H_{19}Cl_2CoN_3$	D / ($g \cdot cm^{-3}$)	1.501
Formula weight	419.2	F(000)	860
Crystal system	Monoclinic	θ range for data collection / (°)	3.33~25.01
Space group	$P2_1/n$	Index range (h, k, l)	$-10 \leqslant h \leqslant 10$, $-13 \leqslant k \leqslant 13$, $-21 \leqslant l \leqslant 20$
a / nm	0.913 70(18)	Total diffraction point	10 381
b / nm	1.160 9(2)	Independent diffraction point (R_{int})	3 268 (0.043 0)
c / nm	1.806 5(4)	Goodness-of-fit on F^2	1.173
β / (°)	104.54(3)	R_1, wR_2 [$I>2\sigma(I)$]	R_1=0.050 9, wR_2=0.098 5
V / nm^3	1.854 8(6)	R_1, wR_2 (all data)	R_1=0.066 4, wR_2=0.103 9
Z	4	Largest diff. peak and hole / ($e \cdot nm^{-3}$)	303 and −394

1.4 DNA binding, DNA cleavage and cytotoxicity experiments

The chemical nuclease activity (absorption spectroscopic assay, fluorescence spectrum assay and pBR322 DNA cleavage activity) and cytotoxicity experiments were conducted using the similar methods described previously[17-18,23]. For complete experimental methods see the Supporting information.

2 Results and discussion

2.1 Description of crystal structure of 1

The crystal structure of complex belongs to the monoclinic system, $P2_1/n$ space group. The crystal analysis results show that the basic unit of the mononuclear cobalt complex is composed of a neutral [Co(L)Cl_2] molecule. As shown in Fig. 1, the Co center of the complex shows a penta-coordinated geometry with N_3Cl_2 donor sets (a tertiary amine N atom, two pyridine N atoms, and two Cl atoms). τ=0.80[22], therefore the coordination center can be described as a trigonal-bipyramidal configuration. Two pyridine N atoms (N2 and N3) and one Cl1 atom occupy the triangular plane position, while the other Cl2 atom and N1 occupy the axial position.

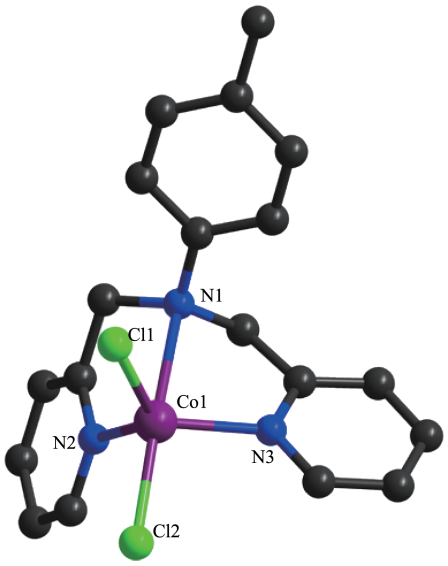

Hydrogen atoms are omitted for clarity

Fig.1 X-ray crystal structure of complex **1**

2.2 DNA-binding studies

The electronic absorption spectrum of the complex interacted with DNA and its corresponding fitting data are shown in Fig. 2a. The observed intense UV absorption peak at 210 nm for the complex are assigned to the π-π^* transition of intraligand. With the gradual addition of CT-DNA, the absorption peak can cause hypochromic effect and a little red shift (7 nm). It can be considered that the complex had an insertion effect with CT-DNA. In order to quantify the insertion capacity of the complex and CT-DNA, the binding constant K_b of interaction of the complex with DNA has been calculated according to the formula $c_{DNA}/(\varepsilon_a-\varepsilon_f)=c_{DNA}/(\varepsilon_b-\varepsilon_f)+1/[K_b(\varepsilon_b-\varepsilon_f)]$ [23]. The relative calculating results are shown in Table S2, and the value of K_b was 9.03×10^4 L·mol^{-1}, which suggests that the binding strength of the complex to DNA is moderate.

As a means for further explore the interaction of the complex with DNA, fluorescence spectra measurements were performed on CT-DNA by varying the concentration of the complex. We used ethidium bromide (EB) as a fluorescent probe and evaluated the binding tendency of the complex to CT-DNA. Fig.2b shows the fluorescence intensity of EB-DNA gradually decreases with the gradual addition of complex, which indicates that the complex can compete with EB to bind DNA. In order to quantitatively calculate the binding capacity to DNA, a straight line should be obtained by plotting the concentration of the quencher with I_0/I according to the classical fluorescence quenching theory (I_0 and I represent the fluorescence intensities in the absence and presence of quencher, respectively). According to the Stern-Volmer equation[24], I_0/I (the ratio of the fluorescence intensity of EB-DNA before and after the addition of the complex) was plotted on the ordinate and the concentration of the complex was taken as the horizon-

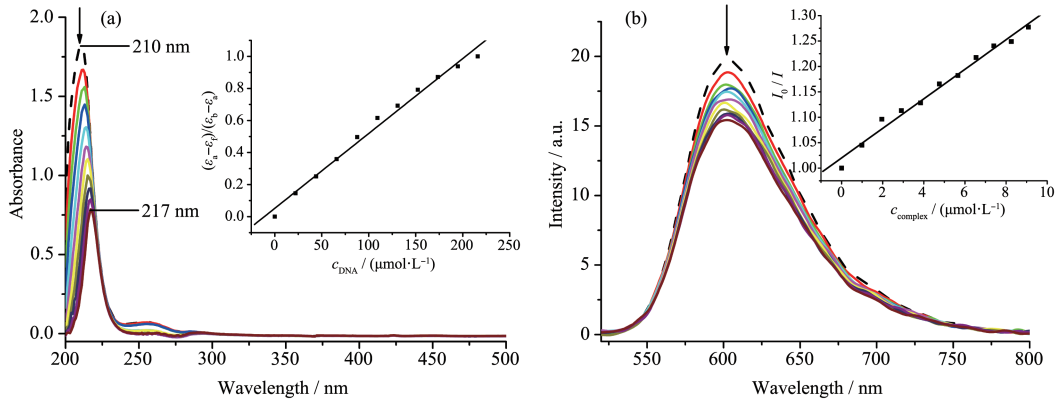

Arrow shows the absorbance changes on increasing DNA concentration; Inset: plot of $(\varepsilon_a-\varepsilon_f)/(\varepsilon_b-\varepsilon_f)$ versus c_{DNA} for the titration of DNA to complex (a) and plot of I_0/I versus the complex concentration (b)

Fig.2 (a) Absorption spectra of complex **1** (2.44 μmol·L^{-1}) in the absence (dashed line) and presence (solid line) of increasing amounts of CT-DNA (22, 44, 66, 88, 109, 131, 152, 174, 195 and 216 μmol·L^{-1}) in 5 mmol·L^{-1} Tris-HCl/50 mmol·L^{-1} NaCl buffer (pH=7.2); (b) Fluorescence emission spectra of EB (2.4 μmol·L^{-1}) bound to CT-DNA (48 μmol·L^{-1}) system in the absence (dashed line) and presence (solid lines) of complex **1** (0.99, 1.96, 2.91, 3.84, 4.76, 5.66, 6.54, 7.41, 8.26 and 9.09 μmol·L^{-1})

tal coordinate. According to the equation $K_{EB}c_{EB}=K_{app}c_{complex}$, $K_{EB}=1.0\times10^7$ L·mol^{-1} ($c_{EB}=2.4$ μmol·L^{-1}), the K_{app} of the complex was calculated to be 7.12×10^5 L·mol^{-1}, which was smaller than the classical bonding constant 10^7 L·mol^{-1} [25]. The results showed that the interaction between the complex and DNA is a medium intercalative mode. It is consistent with the results of electron spectroscopy.

2.3 DNA cleavage studies

2.3.1 Concentration-dependent DNA cleavage activity without any inducer

The covalent closed-loop supercoiled plasmid DNA (SC DNA) is commonly referred to as Form Ⅰ, the open-loop nicked DNA (NC DNA) produced by single-strand cleavage is called Form Ⅱ, and the linear DNA (LC DNA) produced by double-strand cleavage is called Form Ⅲ [26]. In the absence of external agent, the concentration-dependent DNA cleavage activity was performed under the nearly physiological conditions (pH=7.2, 37 ℃, 3 h). The extent of DNA cleavage was estimated by the histogram distribution according to the corresponding gel electrophoresis diagram, which is shown in Fig. 3. The distribution of Form Ⅰ (SC DNA) gradually reduced and that of Form Ⅱ (NC DNA) increased with the increasing concentration of the complex. The complex **1** concentration of 0.65 mmol·L^{-1} (Lane 5) could make DNA produce about 55% of Form Ⅱ. It is demonstrated that the Co(Ⅱ) complex shows certain concentration-dependent DNA cleavage activity without any external agent.

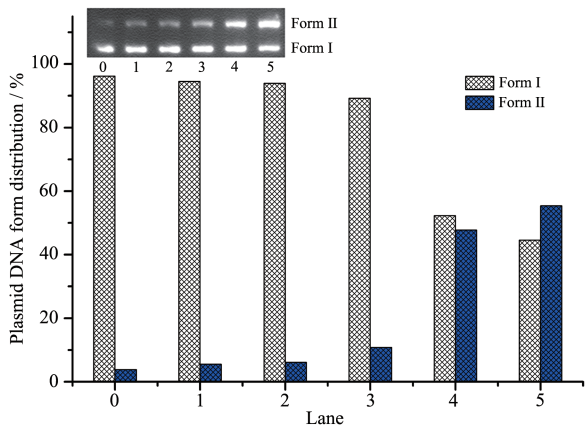

Inset: gel electrophoresis diagrams of pBR322 DNA cleavage activities in Tris-HCl/NaCl buffer (pH=7.2) and 37 ℃ (3 h); Lane 0: DNA control; Lane 1~5: DNA+complex 1 (0.05, 0.2, 0.35, 0.5, 0.65 mmol·L^{-1})

Fig.3 Histogram for cleavage of pBR322 DNA (0.1 μg·μL^{-1}) with complex **1** in the absence of inducer

2.3.2 Concentration-dependent DNA cleavage activity with H_2O_2 as inducer

To further assess the chemical nuclease activity of complex, the concentration-dependent DNA cleavage experiment by complex was also performed in the presence of H_2O_2 under the same physiological conditions (pH=7.2, 37 ℃, 3 h). As shown in Fig. 4, the distribution of Form Ⅰ gradually reduced and Form Ⅱ increased as the concentration changed (0.005~0.05 mmol·L^{-1}). It is worth to mention that the complex could generate about 70% Form Ⅱ from supercoiled plasmid DNA in the presence of H_2O_2 at 0.05 mmol·L^{-1} concentration (Lane 5), while the complex could not induce obvious DNA cleavage without any external agent at the same concentration (Fig.3, Lane 1). The result shows that the DNA cleavage efficiency of complex exhibits remarkable increase due to the addition of H_2O_2.

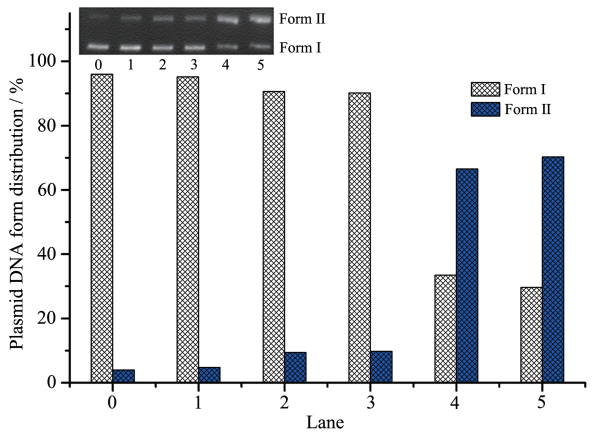

Inset: gel electrophoresis diagrams of pBR322 DNA cleavage activities in Tris-HCl/NaCl buffer (pH=7.2) and 37 ℃ (3 h); Lane 0: DNA control; Lane 1: DNA+0.25 mmol·L^{-1} H_2O_2; Lane 2~5: DNA+H_2O_2+complex 1 (0.005, 0.02, 0.035, 0.05 mmol·L^{-1})

Fig.4 Histogram for cleavage of pBR322 DNA (0.1 μg·μL^{-1}) with complex **1** in the presence of inducer(H_2O_2)

2.3.3 Mechanism of DNA cleavage

In order to further explore the active oxygen species (ROS) which was responsible for the DNA cleav-

age, we have studied several possible inhibitors under aerobic conditions: NaN_3 as singlet oxygen ($^1O_2$) quencher, KI as hydroxyl radical scavenger (·OH), superoxide dismutase (SOD) as O_2^- radical scavenger, catalase as hydrogen peroxide scavenger and EDTA as the chelator of complex. In order to study the binding sites of complex and DNA interactions, we added small groove and large groove binding reagents such as SYBR green and methyl green[27-28].

As shown in Fig.5, the cleavage activity of DNA was significantly inhibited by the addition of the inhibitors NaN_3 (Lane 3) and KI (Lane 4), which indicates that singlet oxygen and hydroxyl radical active species may be produced in the reaction process, and the addition of D_2O (Lane 5) enhanced the cleavage activity of DNA, producing linear DNA, further demonstrating the existence of singlet oxygen active species[29]. In addition, the metal chelating agent EDTA can efficiently inhibit DNA cleavage (Lane 8), indicating metal ion plays the key role in the process of DNA cleavage. Moreover, the addition of methyl green (Lane 9), which is known to interact to DNA at major groove, partly inhibited DNA cleavage by the complex. The result suggests that the complex mainly has interaction with DNA through major groove.

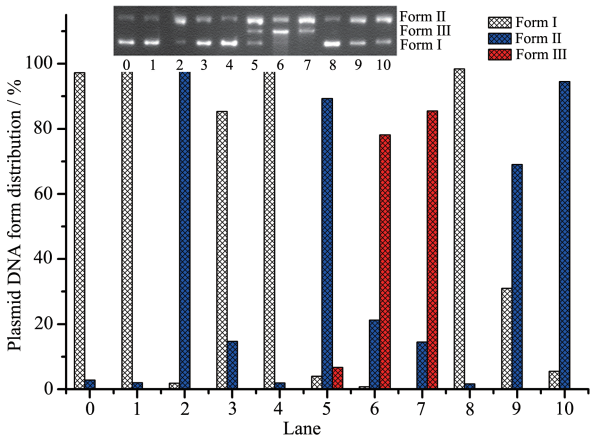

Inset: gel electrophoresis diagrams of pBR322 DNA cleavage activities in Tris-HCl/NaCl buffer (pH=7.2) and 37 ℃ (3 h); Lane 0: DNA control; Lane 1: DNA+0.25 mmol·L^{-1} H_2O_2; Lane 2: DNA+0.25 mmol·L^{-1} H_2O_2+35 μmol·L^{-1} complex **1** (0.07% DMF); Lane 3~10: DNA+0.25 mmol·L^{-1} H_2O_2+complex+inhibitors (1 mmol·L^{-1} NaN_3, 1 mmol·L^{-1} KI, 10% D_2O, 2 U·mL^{-1} SOD, 0.2 U·mL^{-1} Catalase, 0.5 mmol·L^{-1} EDTA, 0.1 mmol·L^{-1} methyl green, 0.15 μL·mL^{-1} SYBR green)

Fig.5 Histogram for cleavage of pBR322 DNA (0.1 μg·μL^{-1}) in presence of 35 μmol·L^{-1} complex **1** and different inhibitors

2.4 Cytotoxicity test

The principle of MTT is that succinate dehydrogenase in mitochondria of living cells can reduce exogenous MTT to water-insoluble blue-purple crystal formazan and deposit in cells, while dead cells have no such function. DMSO can dissolve formazan and measure the absorbance at 490 nm by a microplate reader, which can indirectly reflect the number of living cells. MTT method is often used for screening anti-tumor drugs, cytotoxicity test and radiosensitivity test. Cytotoxicity is usually measured by the IC_{50} value. We used the MTT method to determine the inhibitory ability of the complex on the growth of HeLa, BGC-823 and NCI-H460 cells *in vitro* (Table 2), and the IC_{50} values were (243.27±7.82), (148.54±5.76) and (234.24±7.07) μmol·L^{-1}, respectively. In addition, the cell viability of three cell lines after drug treatment for 48 h by complex have been shown in Fig.6, and the result indicates that the complex is cytotoxic and inhibit the growth of cells in a dose-dependent manner. We found that the ligand itself showed very weak inhibitory effects on three cell lines. The results show that the complex has a certain degree of inhibition on cancer cells, and especially has a significant inhibition on BGC-823 cells.

Table 2 IC_{50} values of complex 1 obtained with different cell lines for 48 h

Compound	IC_{50} / (μmol·L^{-1})		
	HeLa	BGC-823	NCI-H460
Cisplatin	23.07±1.64	2.23±0.14	16.31±0.05
$[Co(L)Cl_2]$	243.27±7.82	148.54±5.76	234.24±7.07
L	>500	>300	>400

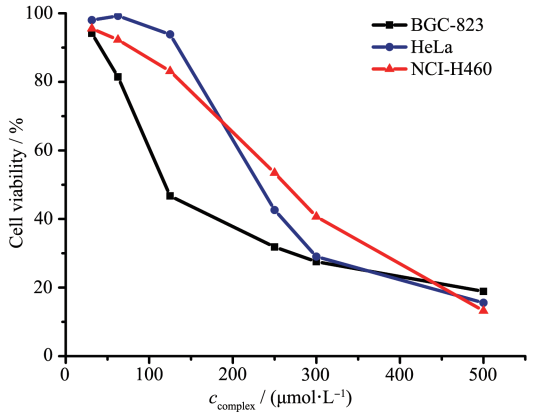

Fig.6　Cell viability of three cell lines (BGC-823, HeLa and NCI-H460) after drug treatment for 48 h by complex **1**

3　Conclusions

A new polypyridyl mononuclear Co(Ⅱ) complex was synthesized and characterized using elemental analysis, IR, and X-ray crystallography techniques. The crystal structure analysis reveals that Co(Ⅱ) center of the complex is a distorted trigonal-bipyramidal configuration. Electronic spectra and fluorescence quenching experiments show a moderate insertion between the complex and CT-DNA. The DNA cleavage ability of the complex exhibits evident improvement after the addition of the inducer H_2O_2. The oxidative mechanism is demonstrated preliminarily via a pathway involving formation of both singlet oxygen ($^1O_2$) and hydroxyl radicals (·OH) as active oxygen species. In addition, *in vitro* cytotoxicity of the drug has been tested by MTT against HeLa, BGC-823 and NCI-H460 cell lines, and the result shows that the complex has certain inhibitory effects on the three cancer cells.

Acknowledgements: This work was supported by Shanxi Key Research and Development Program (Grants No.201703D211001-02-03, 201903D221036, 201703D221008-4, 201703D221004-5), Natural Science Foundation of Shanxi (Grants No. 201701D221157, 201701D221158), the PhD Research Startup Foundation of Shanxi Agricultural University (Grant No. 2013YJ40) and College Students Innovation and Entrepreneurship Training Project of Shanxi (Grants No.2019136, 2019137).

Supporting information is available at http://www.wjhxxb.cn

References:

[1] Komor A C, Barton J K. *Chem. Commun.*, **2013**,**49**(35):3617-3630

[2] Barton J K. *Comments Inorg. Chem.*, **1985**,**3**(6):321-348

[3] Liu Y, Chouai A, Degtyareva N N, et al. *Chem. Rev.*, **1998**,**98**(3):1109-1152

[5] Galal S A, Hegab K H, Kassab A S, et al. *Eur. J. Med. Chem.*, **2009**,**44**(4):1500-1508

[6] Kumar P, Baidya B, Chaturvedi S K, et al. *Inorg. Chim. Acta*, **2011**,**376**(1):264-270

[7] Ghosh K, Tyagi N, Kumar H, et al. *Spectrochim. Acta A*, **2015**, **146**:292-296

[8] Smolková R, Zeleňák V, Gyepes R, et al. *Polyhedron*, **2018**, **141**:230-238

[9] Srishailam A, Gabra N M, Kumar Y P, et al. *J. Photochem. Photobiol. B*, **2014**,**141**:47-58

[10]Xu X M, Yao J H, Mao Z W, et al. *Inorg. Chem. Commun.*, **2004**,**7**(6):803-805

[11]He J, Hu P, Wang Y J, et al. *Dalton Trans.*, **2008**(24):3207-3214

[12]Du K J, Wang J Q, Kou J F, et al. *Eur. J. Med. Chem.*, **2011**, **46**(4):1056-1065

[13]Balakrishnan N, Haribabu J, Anantha Krishnan D, et al. *Polyhedron*, **2019**,**170**:188-201

[14]Munteanu C R, Suntharalingam K. *Dalton Trans.*, **2015**,**44**(31):13796-13808

[15]Yamada K. *Interrelations between Essential Metal Ions and Human Diseases*. Sigel A, Sigel H, Sigel R K O. Ed., Dordrecht: Springer, **2013**:295-317

[16]Randaccio L, Geremia S, Nardin G, et al. *Coord. Chem. Rev.*, **2006**,**250**(11/12):1332-1350

[17]Gao C Y, Ma Z Y, Zhang Y P, et al. *RSC Adv.*, **2015**,**5**(39): 30768-30779

[18]Zhang Y P, Ma Z Y, Gao C Y, et al. *New J. Chem.*, **2016**,**40**(9):7513-7521

[19]Sheldrick G M. *Correction Software*, University of Göttingen, Germany, **1996**.

[20]Sheldrick G M. *SHELXS*-97, *Program for Crystal Structure Resolution*, University of Göttingen, Germany, **1997**.

[21]Sheldrick G M. *SHELXL*-97, *Program for Crystal Structures Analysis*, University of Göttingen, Germany, **1997**.

[22]Addison A W, Rao T N, Reedijk J, et al. *Dalton Trans.*, **1984**,**7**:1349-1356

[23]Gao C Y, Qiao X, Ma Z Y, et al. *Dalton Trans.*, **2012**,**41**(39): 12220-12232

[24]Sung J, Shin K J, Lee S. *Chem. Phys.*, **1992**,**167**(1/2):17-36

[25]Patra A K, Dhar S, Nethaji M, et al. *Dalton Trans.*, **2005**(5): 896-902

[26]Kellett A, Molphy Z, Slator C, et al. *Chem. Soc. Rev.*, **2019**, **48**:971-988

[27]Gibellini D, Vitone F, Schiavone P, et al. *J. Clin. Virol.*, **2004**,**29**:282-289

[28]ElAmrani F B, Perelló L, Real J A, et al. *J. Inorg. Biochem.*, **2006**,**100**:1208-1218

[29]Merkel P B, Kearns D R. *J. Am. Chem. Soc.*, **1972**, **94**(3): 1029-1030